The International Journal of Cardiovascular Imaging (2006) 22: 407–416
DOI 10.1007/s10554-005-9031-1

Clinical validation of the gated blood pool SPECT QBS® processing software in congestive heart failure patients: correlation with MUGA, first-pass RNV and 2D-echocardiography

Marcus Hacker[1], Xaver Hoyer[1], Sandra Kupzyk[1], Christian La Fougere[1], Johann Kois[1], Hans-Ulrich Stempfle[2], Reinhold Tiling[1], Klaus Hahn[1] & Stefan Störk[3]

[1]*Department of Nuclear Medicine, University of Munich, Munich, Germany;* [2]*Department of Cardiology, University of Munich, Munich, Gemany;* [3]*Cardiology, University of Würzburg, Würzburg, Germany*

Received 6 April 2005; accepted in revised form 29 August 2005

Key words: echocardiography, gated blood pool SPECT, heart failure, radionuclide ventriculagraphy

Abstract

Introduction: Left (LVEF) and right ventricular ejection fraction (RVEF) as well as LV regional wall motion at rest are valuable tools to monitor and tailor treatment of congestive heart failure (CHF) patients. Gated blood pool SPECT (GBPS) is under evaluation as an ''all-in-one'' technique, providing information on LVEF, RVEF, and wall motion derived from a single examination. Aim of the study was to evaluate a commercially available automated GBPS processing software for EF measurements and wall motion analysis in heart failure patients. *Methods*: Thirty-two patients (12 female; mean age ± SD: 53 ± 13 years), suffering from dilated (63%), ischemic (25%) or hypertrophic (13%) cardiomyopathy, were studied. First-pass radionuclide ventriculography (FP-RNV), planar multigated radionuclide angiography (MUGA), and GBPS were performed at rest after *in vivo* labeling of red blood cells, and LVEF and RVEF was calculated with each method. Later on the same day LVEF was calculated by echocardiography. LV wall motion (summed motion score and wall motion index) was derived from GBPS and echocardiography using the standard 16-segment model. *Results*: Mean LVEF measured by GBPS, echocardiography, MUGA and FP-RNV was 33 ± 13%, 37 ± 15%, 41 ± 14% and 45 ± 13%, respectively. LVEF values calculated from GBPS showed moderate to good correlation with FP-RNV ($r = 0.61$), MUGA ($r = 0.65$) and ECHO ($r = 0.74$; all $p < 0.01$). Mean RVEF calculated by GBPS, FP-RNV and MUGA was 45 ± 14%, 46 ± 9% and 38 ± 9%, respectively. RVEF values calculated from GBPS showed weak correlation with FP-RNV ($r = 0.33$) and MUGA ($r = 0.26$; all $p =$ n.s.). Assessment of GBPS wall motion was qualitatively possible in all patients. The agreement between GBPS and ECHO was 82% ($\kappa = 0.73$). The wall motion index showed good correlation between both methods ($r = 0.88$; $p < 0.001$). *Conclusion*: An automated algorithm for LVEF calculation and wall motion analysis using GBPS is feasible for clinical routine diagnostic in CHF patients. The RVEF calculation method needs to be improved before routine clinical application can be recommended.

Abbrevations: CHF – congestive heart failure; FP-RNV – first-pass radionuclide ventriculography; GBPS – gated blood pool SPECT; LVEF – left ventricular ejection fraction; MRI – magnetic resonance imaging; MUGA – multigated radionuclide angiography; ROI – region of interest; RVEF – right ventricular ejection fraction

Introduction

Both monitoring and tailoring of therapy in chronic heart failure (CHF) patients is aided by precise measurements of left (LVEF) and right ventricular ejection fraction (RVEF) as well as LV regional wall motion. These parameters have also been shown to play an important role as prognostic determinants [1–8]. Over the years, several imaging modalities have been developed which vary considerably regarding precision, ease of use, availability, and costs. LVEF may be measured by radiographic contrast angiography, cardiac magnetic resonance imaging (MRI), two- and three-dimensional echocardiography and different radionuclide methods like gated blood pool single positron emission computer tomography (GBPS), planar multigated radionuclide angiography (MUGA), or first-pass radionuclide ventriculography (FP-RNV). Two- or three-dimensional wall motion analysis can also be measured by most of these methods, and, in addition, RVEF can be calculated by MRI, FP-RNV and MUGA.

To date, there is no "all-in-one" method used in clinical routine, providing left and right ventricular parameters to monitor CHF patients. In theory, GBPS offers this advantage because it is easily performed, it diffenrentiates LV and RV without overlap of other cardiac chambers by its tomographic perspective thus facilitating precise measurement, and it allows sophisticated wall motion analysis, all within one examination [9–16].

Regarding LVEF, numerous studies have described a good correlation between GBPS, MUGA and FP-RNV [13, 17–22]. Furthermore, a good correlation was reported for LV and RV parameters between GBPS and MRI [11, 15]. However, since image processing was complicated and time consuming, GBPS did not find widespread clinical acceptance. Recently, fully automated software programs for GBPS processing have been developed and are now commercially available. Using these programs, excellent correlation with MUGA [23–25], MRI [26] and a biventricular dynamic physical phantom [27] was documented delivering highly reproducible and accurate LVEF values. Good correlation was also found for RV parameters compared with FP-RNV [28] and MRI [26]. First experiences with regional wall motion analysis were encouraging [16].

The aim of the present study was to assess the clinical utility of a commercially available automated GBPS processing software (QBS®, Cedars-Sinai Medical Center, Los Angeles, USA), introduced by Kriekinge et al. [25], in the setting of clinical routine diagnostics. EF measurements and wall motion analysis derived from GBPS were compared to MUGA, FP-RNV and two-dimensional echocardiography in CHF patients.

Methods

Chronic Heart Failure Patients

Consecutive CHF patients from our heart failure outpatient clinics who were hospitalized to optimize their medical treatment and/or to assess the need for heart transplantation were eligible if their GBPS, FP-RNV, MUGA, and echocardiography examinations had been performed on the same day. In total, 32 patients, 20 men and 12 women, were included in the study and their characteristics are listed in Table 1. In a pre-selection examination, three patients were excluded for correlation of wall motion analysis owing to the fact that less than 12 segments were clearly detectable by echocardiography.

Radionuclide Ventriculography

RNV studies were performed at rest by *in vivo* red blood cell labeling. Sn-Agens was injected intravenously. After 20 min patients were placed upright in front of a Picker SIM 400 multicrystal camera, equipped with a low energy high sensitivity parallel hole collimator in approximately 30° RAO projection. 740 MBq technetium 99 m pertechnetate was injected. The camera acquired a total of 1500 frames at 25 ms/frame. Initial LV and RV regions of interest (ROI) were drawn and the time-activity curves generated. Start and stop of the RV and LV phase and first identifiable beats were defined and the ROIs modified through iterative steps by the

Table 1. Patient characteristics of the study cohort ($n = 32$). Values are mean (SD), unless indicated otherwise.

Characteristic	
Age, years	53 (13)
Female, *n* (%)	12 (38)
Body mass index, kg/m^2	27.3 (4.8)
Cardiac diagnosis: Ischemic heart disease, *n* (%)	8 (25)
Dilated cardiomyopathy, *n* (%)	20 (63)
Hypertrophic cardiomyopathy, *n* (%)	4 (13)
NYHA class: II, *n* (%)	27 (84)
III, *n* (%)	3 (10)
IV, *n* (%)	2 (6)
Atrial fibrillation, *n* (%)	4 (13)
Pacemaker, *n* (%)	8 (25)
Left bundle branch block, *n* (%)	6 (19)

NYHA = New York Heart Association.

computer software. Borders of the RV and LV end-diastolic regions were determined from the phase images and the end-systolic difference images. The phase images were used to identify valve planes. The end-systolic regions were drawn from the end-systolic images. FP-LVEF was calculated by dual ROI method. FP-RVEF was calculated using a single end-diastolic frame (single ROI method).

After the FP acquisition, patients were positioned supine on a scanning couch for planar MUGA acquisition. A Picker Prism 2000 or Picker Axis gamma camera equipped with a low energy high resolution collimator was set in 40° LAO projection (“best septal view”). LVEF and RVEF were calculated by dual ROI method. The background ROI was placed adjacent to the free wall of the ventricles.

Gated blood pool SPECT

Immediately after obtaining the planar views, GBPS was performed using the same cameras described above with the two detectors in 180° configuration. Acquisition parameters for GBPS consisted of 30 steps per 180°, 60 s per step, 8 frames per cardiac cycle, 64×64 matrix, step and shoot mode, an energy window of 15% centered on 140 keV, and a R–R acceptance window of ±15%. Studies were reconstructed by ramp-filtered back-projection using a 3D post-filter (low pass 8.0/0.32). Short-axis datasets were generated by manual reorientation.

GBPS was processed using the fully automated QBS® algorithm as described elsewhere [25, 28]. In case of implausible identification of ventricle borders the QBS® software allows to manually adjust LV and RV ROIs by shifting an ellipsoid over the LV (Figure 3a). Accordingly, LVEF was calculated using the maximum diastolic and systolic dispersion of the LV. For RVEF calculation, the dispersion of the RV according to the LV phases was used without further adjustment of LV and RV ROIs. In case of a phase shift between LV and RV, the visually maximally dispersed end-diastolic and end-systolic images of the RV were used to calculate RVEF manually.

LV wall motion from the QBS® images was assessed visually using cine loops with maximal end-diastolic dispersion. The reader was allowed to rotate the beating cine display into any angle for best assessment of a particular cardiac region. A standard 16 segment model, four point score (1 = normal; 2 = hypokinetic; 3 = akinetic; 4 = dyskinetic) was used for both QBS® and echocardiographic data to enable direct comparison of the same areas. The sum of the 16 motion scores was defined as summed motion score (SMS), and a wall motion index (WMI) was calculated as SMS per number of segments analysed.

Two-dimensional echocardiography

Later on the same day, two-dimensional M-mode resting echocardiography was performed according to the recommendations of the American Society of Echocardiography with apical 4-, 2- and 3-chamber views, parasternal long axis (i.e., parasternal 3-chamber view) and parasternal short axis at base, mid and apical position (Philips HP Sonos 5500, Andover, Mass., USA or GE Vingmed System V, Horten, Norway). LV cavity dimensions at end-systole and end-diastole were measured (modified Simpson’s method: biplane planimetry from apical 4- and 2-chamber view) [29–35] and LVEF was calculated from the volume data. Wall motion was analyzed according to the same 16-segment model and procedure as described above. Segments which could not be delineated clearly by the reader were not included in the analysis.

Reading procedure

All measurements from GBPS, MUGA, FP and echocardiographic recordings were performed off-line by different experts (MH, CLF, JK and XH) blinded to the results of complementary readings.

Data analysis

Results are presented as mean ± standard deviation (SD), unless stated otherwise. The different imaging modalities were compared using Mann Whitney-*U* and Wilcoxon tests as appropriate. Bland–Altman plots were inspected to visually assess the association between measurements from different methods. The between-method agreement was estimated using weighted kappa statistics (κ). The κ provides an estimate for the strength of agreement between two categorical variables taking into account the agreement which may have occurred by chance. The κ may be graded as <0.20, very bad agreement; 0.21–0.40, bad; 0.41–0.60, fair; 0.61–080, good; 0.81–1.00, very good. Spearman's coefficient (r) is given when correlations are reported. The level of statistical significance was set at less than 5%.

Results

LVEF

For LVEF calculation using GBPS, automatic ROI fitting with QBS® was successful in 81% (26/32) of patients; the remaining patients were processed using the manual option in QBS®. Mean LVEF values measured by GBPS, echocardiography, MUGA and FP-RNV were 33 ± 13%, 37 ± 15%, 41 ± 14% and 45 ± 13%, respectively. Single LVEF values calculated from GBPS showed moderate to good correlation with MUGA ($r=0.65$), FP-RNV ($r=0.61$) and echocardiography ($r=0.74$; all $p<0.001$). However, GBPS delivered statistically significant lower values compared to all other methods (Table 2) and the Bland–Altman plot showed underestimation for GBPS-LVEF values compared to MUGA, FP-RNV, and echocardiography (Figure 1).

RVEF

For RVEF calculation using GBPS, the QBS® automatically fitting algorithm was successful in 81% (26/32) of patients; the remaining patients were processed manually by moving the LV ellipsoid to obtain the visually best fitting RV contours. Mean RVEF calculated by GBPS, FP-RNV and MUGA was 45 ± 14%, 46 ± 9% and 38 ± 9%, respectively. RVEF values calculated from GBPS showed weak correlation with FP-RNV ($r=0.33$, Figure 2) and MUGA ($r=0.26$; all $p=$ n.s.). The Bland-Altman plot for RVEF values measured from GBPS and FP-RNV showed a tendency for an overestimation of higher RVEF values with GBPS (Figure 2).

Wall motion analysis

29/32 (91%) patients showed 12 or more detectable segments in echocardiography and were considered for wall motion analysis. 431/464 (93%) segments in echocardiography and 464/464 (100%) segments in GBPS could be analysed. Of the 431 segments analyzed by both methods, 174 (40%) revealed normal wall motion in GBPS, 171 (40%) showed hypokinesia and 86 (20%) segments showed akinesia or dyskinesia. In echocardiography, 170 (40%) segments revealed normal wall motion, 159 (37%) showed hypokinesia and 93 (22%) akinesia or dyskinesia. The agreement between both

Table 2. Left and right ventricular ejection fractions as assessed by different methods. Values are mean ± SD [range]. *p* values for GBPS value vs. complementary methods (Wilcoxon test).

	LVEF (%)	*p*	RVEF (%)	*p*
GBPS	33 ± 13 [9;59]		45 ± 14 [19;78]	
FP-RNV	45 ± 13 [22;67]	< 0.0001	46 ± 9 [19;67]	0.554
MUGA	41 ± 14 [16;68]	0.001	38 ± 9 [17;58]	0.028
Echocardiography	37 ± 15 [11;70]	0.004	–	–

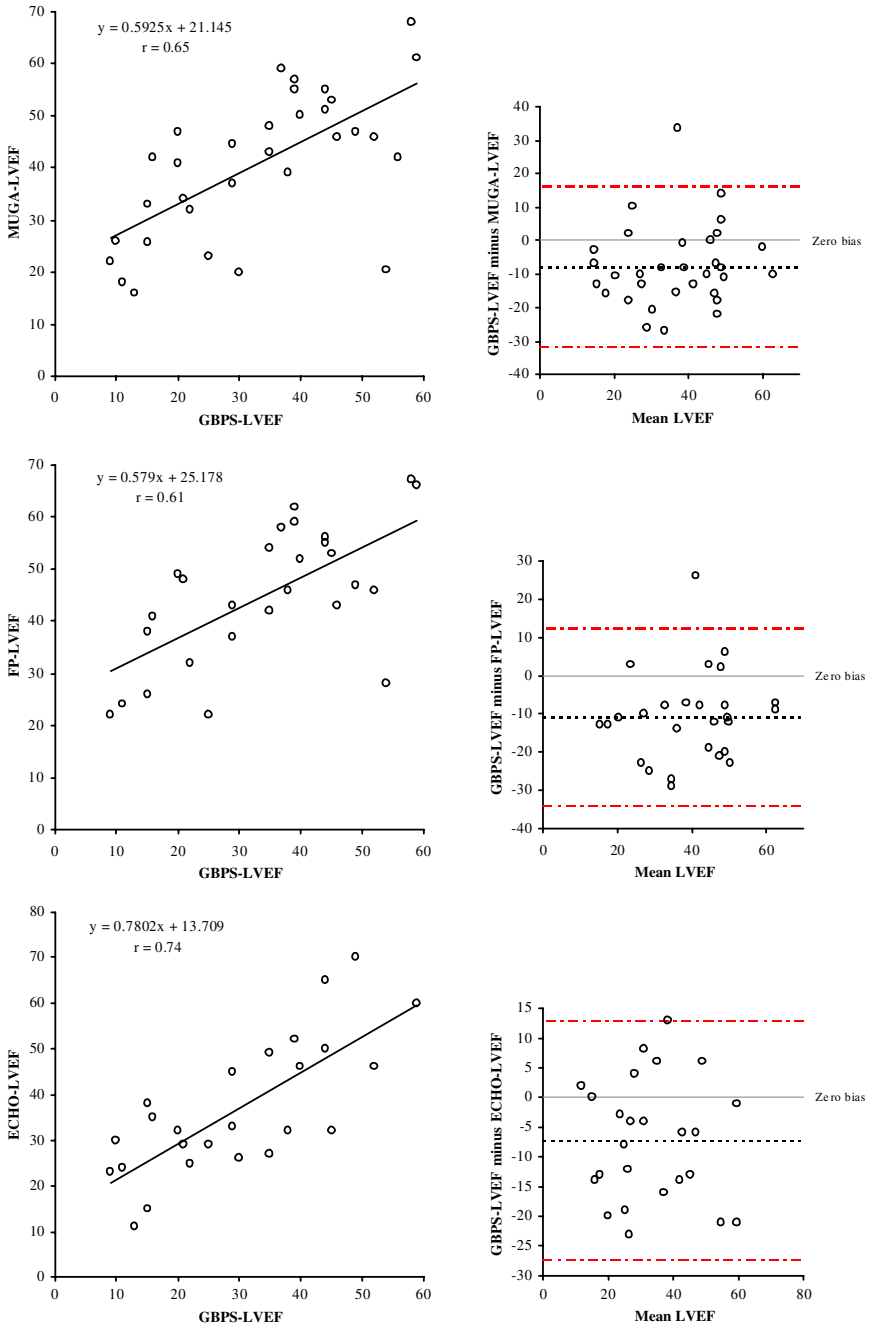

Figure 1. Scatter plot and Bland-Altman plot for different LVEF calculation modalities. Upper panel: GBPS-QBS® vs. MUGA ($n = 32$); the bias (95% limits) detected by the Bland-Altman approach was −7.7 (−31.7; 16.3). Middle panel: GBPS-QBS® vs. FP-RNV ($n = 25$); bias (95% limits) was −7.2 (−27.3; 12.9). Lower panel: GBPS-QBS® vs. echocardiography ($n = 27$); bias (95% limits) was −10.7 (−33.8; 12.4).

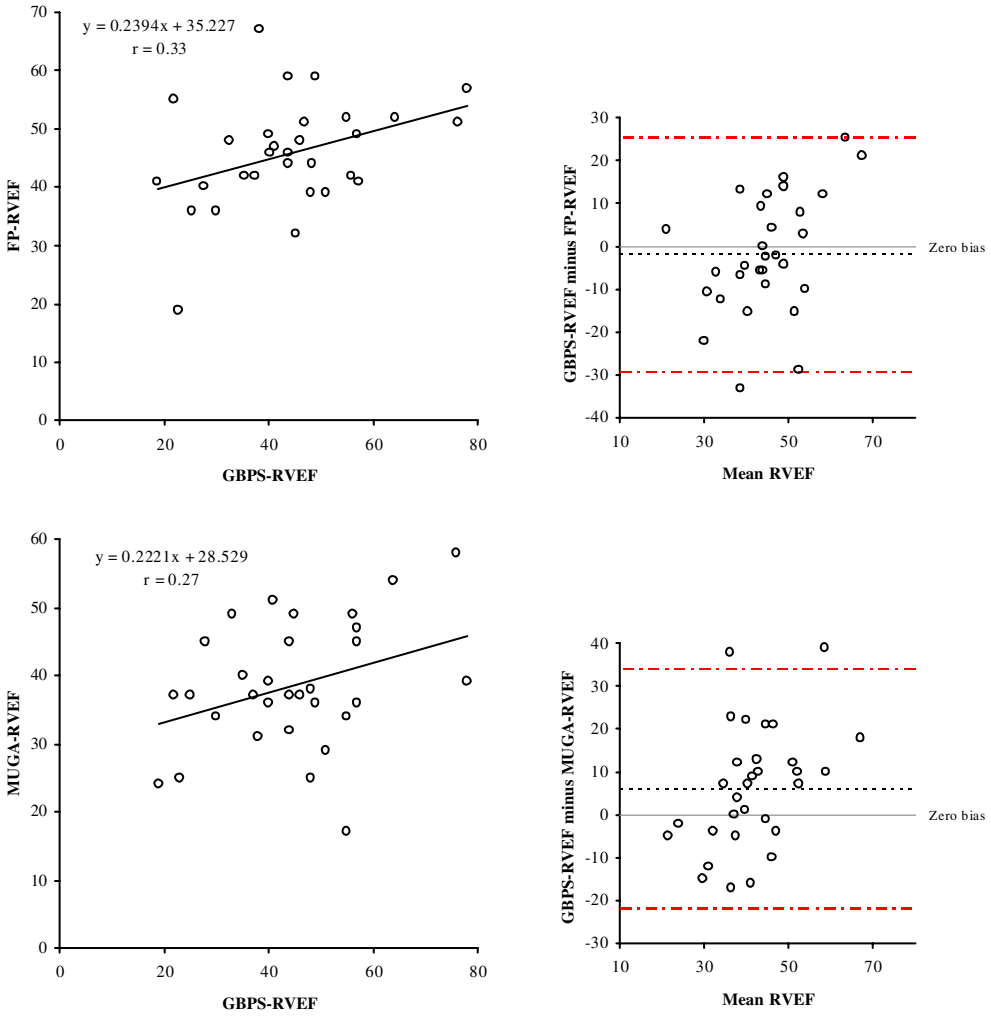

Figure 2. Scatter plot and Bland-Altman plot for different RVEF calculation modalities. Upper panel: GBPS-QBS® vs. FP-RNV ($n = 30$); the bias (95% limits) detected by the Bland–Altman approach was −1.7 (−29.1; 25.6). Lower panel: GBPS-QBS® vs. MUGA ($n = 31$); bias (95% limits) was 6.2 (−21.7; 34.1).

methods is demonstrated in Table 3 on a segmental basis. An exact overall agreement of 82% was found, with $\kappa = 0.73$ indicating good agreement. Furthermore, the WMI showed a good correlation between both methods ($r = 0.88$; $p < 0.0001$).

Discussion

To our knowledge, this is the first study which describes the clinical utility of the QBS® software for GBPS as an "all-in-one" tool for the evaluation of LV and RV function and regional wall motion analysis. LV and RV parameters were compared with the results from MUGA, FP-RNV and echocardiography, considering MUGA as the reference standard for LVEF, FP-RNV for RVEF, and echocardiography for wall motion analysis.

LVEF

In the present study, moderate to good correlation of the single LVEF values was found between

Table 3. Agreement of regional wall motion analysis between echocardiography and GBPS. 1, normal wall motion; 2, hypokinesia; 3–4, akinesia or dyskinesia.

GBPS	Echocardiography		
	1	2	3–4
1	149	17	8
2	23	133	15
3–4	7	9	70

Overall agreement was 82%, the weighted kappa statistic was 0.73.

GBPS and other calculation modalities. This is in accordance with previous studies describing both good correlation and high reproducibility of LVEF meaurements assessed by GBPS with other methods [11, 13, 17–22]. However, LVEF values calculated from GBPS were significantly lower compared to all other modalities. There is scarce published data using the QBS® processing software for evaluating patients with compromised LV function. Wright et al. reported good correlation between LVEF calculated from GBPS-QBS® and MUGA in 50 patients with permanent pacemaker and an echocardiographic LVEF ≤40% [36]. The success rate of the automated algorithm with 70% was relatively poor in that study whereas the present study delivered a higher success rate of 81%. Wright et al. explained the low automatic contour finding rate in their study by pacemaker induced ventricular dyssynchrony, and the QBS® algorithm was not able to automatically resolve this problem. In addition, in the present study, the QBS® algorithm was not flexible enough in differentiating the base of the LV from the left atrium which is relevant in CHF patients with mitral regurgitation.

However, also in patients with normal LVEF values the published results for GBPS compared to MUGA are inconsistent. In accordance with the present study, Nichols et al. found significantly lower LVEF values from GBPS compared to MUGA in a retrospective analysis of 422 patients [26]. That study also showed that normal limits for GBPS-QBS® were significantly lower than for MRI. The authors concluded that separate normal limits for GBPS calculations are needed for correct interpretation of measurements. By contrast, Daou et al. reported significantly higher LVEF values calculated from GBPS-QBS® compared to MUGA in 29 male patients, assuming atrial overlap in MUGA [24]. Both studies investigated heterogenous patient populations including patients after heart transplantation or chemotherapy, and patients with primary arterial hypertension, coronary artery disease and previous myocardial infarction but only a small number of heart failure patients with compromised LV function.

An underestimation of LV values of 8-frame studies compared to 16-frame studies has been demonstrated using gated myocardial perfusion SPECT [37] while Kim et al. could not find statistically significant differences in LVEF volumes for GBPS comparing eight and 16 frame studies in a heterogenous collective of 66 patients [38]. Adachi et al. reported no significant differences in LVEF between 180° and 360° orbit acquisition in nine healthy controls and 34 patients with different cardiomyopathies [39]. Further studies are needed to clarify these issues in GBPS imaging particulary in heart failure patients with markedly reduced LVEF.

RVEF

Mean RVEF calculated from GBPS-QBS® was in the same range compared to FP-RVEF (45% vs. 46%) and higher than MUGA-RVEF (38%). Planar MUGA in LAO projection tends to underestimate RVEF if there is major overlap of right atrium (RA) and RV, which is common in CHF [40]. Correlation among RVEF values was weak ($r = 0.33$), which is in line with data from Slart et al. who analysed the GBPS results of 22 patients with a different software package and found a correlation of $r = 0.40$ [41]. Conversely, Daou et al. found a good correlation ($r = 0.68$) between QBS® -RVEF and FP-RVEF in 64 patients with chronic postembolic pulmonary hypertension [28]. However, this study excluded 25% of patients because of unsuccessful FP-RNV, while in the present study only 6% had to be excluded. The preselection of suitable FP-RVEF, usually because of fractioned or diffuse bolus transit, may have led to strengthened but overoptimistic correlation in that study. However, strong correlation between RVEF assessed

with a different automated GBPS algorithm and MRI ($r = 0.85$) was already reported by Nichols et al., who investigated 28 patients with primary arterial hypertension or tetralogy of Fallot [26]. In the present study, the success rate of the automated QBS® algorithm was in a similar range compared to LVEF measurements. However, automated contour finding results were not only hampered by difficulties to separate the valve plane area from the right atrium as described above for the left ventricle. In addition, unsatisfactory results of the automated QBS® algorithm frequently could not be improved by manual adjustments because the current version of the QBS® software does not allow to draw separate contours around the RV. This may be the major limitation explaining the weak RVEF correlation between FP-RNV and GBPS-QBS® in the present study (Figure 3).

Wall motion analysis

In the present study, GBPS acquisition and processing for segmental wall motion analysis with QBS® was feasible in all patients including those three patients in whom echocardiography was not interpretable, if less than 12 segments in quantitative analysis were clearly detectable. By contrast, echocardiography delivers additional prognostic parameters which cannot be derived from GBPS as the degree of wall thickening and valve analysis.

A good overall agreement of 82% ($\kappa = 0.73$) was found regarding the 431 segments that could be analyzed in both methods. This is consistent with previous studies comparing regional wall motion assessed by gated myocardial SPECT with the results of echocardiography [29, 42]. The agreement in those studies varied between 68 and 69%. Despite the diffuse muscular involvement in dilated cardiomyopathy segmental wall motion abnormalities are frequent, and are associated with systolic dysfunction and a worse prognosis [8, 43]. In the present study, 63% of patients suffered from idiopathic dilated cardiomyopathy and segmental analysis for GBPS and echocardiography was performed particularly careful by two independent

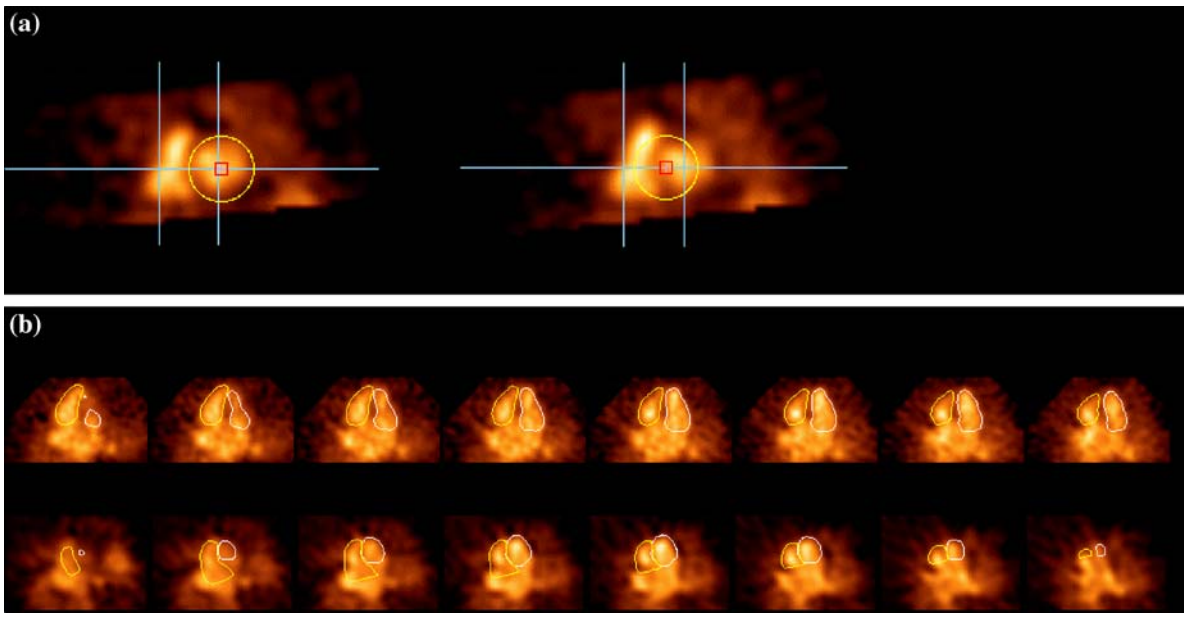

Figure 3. Example of QBS®edge detection. (a) Manual adjustment of left ventricular edge detection, shifting an ellipsoid over the left ventricle (left). For the manual adjustment of the contours of the right ventricle, only the left ventricular ellipsoid can be adjusted (right). (b) Coronal view of end-diastolic images showing left (white) and right ventricular contours (yellow) after manual adjustment. Successful edge detection of the right ventricle is shown in the upper row; by contrast, in the lower row, the right ventricular contours are displaced into the right atrial area.

observers in patients with global wall motion reduction, a fact that might explain the good overall agreement. Segmental disagreement was predominantely caused by either image artifacts in GBPS or allocation of areas with reduced wall motion to differing segments by the two observers.

Study limitations

The QBS® software for automated GBPS processing requires no operator intervention, but if adjustments are needed, there are no possibilities for drawing RV contours manually, so that inaccuracies might result for RVEF calculation in some patients. Moreover, QBS® software is not considering phase shifting between LVEF and RVEF for automated RVEF calculation. Care was taken to manually calculate RVEF from maximum end-diastolic and maximum end-systolic frames in these cases.

Conclusion

The automated QBS® algorithm for LVEF calculation and wall motion analysis using GBPS is feasible for clinical routine diagnostic in CHF patients but tends to underestimate LVEF values. The RVEF calculation method needs to be improved before routine clinical application can be recommended.

References

1. de Groote P, Millaire A, Foucher-Hossein C, et al. Right ventricular ejection fraction is an independent predictor of survival in patients with moderate heart failure. J Am Coll Cardiol 1998; 32: 948–954.
2. Effect of enalapril on survival in patients with reduced left ventricular ejection fractionsand congestive heart failure. The SOLVD Investigators. N Engl J Med 1991; 325: 293–302.
3. Hughes CV, Wong M, Johnson G, Cohn JN. Influence of age on mechanisms and prognosis of heart failure. The V-HeFT VA Cooperative Studies Group. Circulation 1993; 87: VI111–117.
4. Cohn JN, Johnson GR, Shabetai R, et al. Ejection fraction, peak exercise oxygen consumption, cardiothoracic ratio, ventricular arrhythmias, and plasma norepinephrine as determinants of prognosis in heart failure. The V-HeFT VA Cooperative Studies Group. Circulation 1993; 87: VI5–16.
5. Gradman A, Deedwania P, Cody R, et al. Predictors of total mortality and sudden death in mild to moderate heart failure. Captopril-Digoxin Study Group. J Am Coll Cardiol 1989; 14: 564–570. discussion 571–562.
6. Di Salvo TG, Mathier M, Semigran MJ, Dec GW. Preserved right ventricular ejection fraction predicts exercise capacity and survival in advanced heart failure. J Am Coll Cardiol 1995; 25: 1143–1153.
7. Parameshwar J, Keegan J, Sparrow J, Sutton GC, Poole-Wilson PA. Predictors of prognosis in severe chronic heart failure. Am Heart J 1992; 123: 421–426.
8. Fauchier L, Eder V, Casset-Senon D, et al. Segmental wall motion abnormalities in idiopathic dilated cardiomyopathy and their effect on prognosis. Am J Cardiol 2004; 93: 1504–1509.
9. Vanhove C, Franken PR. Left ventricular ejection fraction and volumes from gated blood pool tomography: comparison between two automatic algorithms that work in three-dimensional space. J Nucl Cardiol 2001; 8: 466–471.
10. Vanhove C, Franken PR, Defrise M, Momen A, Everaert H, Bossuyt A. Automatic determination of left ventricular ejection fraction from gated blood-pool tomography. J Nucl Med 2001; 42: 401–407.
11. Chin BB, Bloomgarden DC, Xia W, et al. Right and left ventricular volume and ejection fraction by tomographic gated blood-pool scintigraphy. J Nucl Med 1997; 38: 942–948.
12. Bartlett ML, Srinivasan G, Barker WC, Kitsiou AN, Dilsizian V, Bacharach SL. Left ventricular ejection fraction: comparison of results from planar and SPECT gated blood-pool studies. J Nucl Med 1996; 37: 1795–1799.
13. Faber TL, Stokely EM, Templeton GH, Akers MS, Parkey RW, Corbett JR. Quantification of three-dimensional left ventricular segmental wall motion and volumes from gated tomographic radionuclide ventriculograms. J Nucl Med 1989; 30: 638–649.
14. Links JM, Becker LC, Shindledecker JG, et al. Measurement of absolute left ventricular volume from gated blood pool studies. Circulation 1982; 65: 82–91.
15. Nichols K, Saouaf R, Ababneh AA, et al. Validation of SPECT equilibrium radionuclide angiographic right ventricular parameters by cardiac magnetic resonance imaging. J Nucl Cardiol 2002; 9: 153–160.
16. Eder V, Bernis F, Drumm M, Diarra MI, Baulieu F, Leger C. Three-dimensional analysis of left ventricle regional wall motion by using gated blood pool tomography. Nucl Med Commun 2004; 25: 971–978.
17. Calnon DA, Kastner RJ, Smith WH, Segalla D, Beller GA, Watson DD. Validation of a new counts-based gated single photon emission computed tomography method for quantifying left ventricular systolic function: comparison with equilibrium radionuclide angiography. J Nucl Cardiol 1997; 4: 464–471.
18. Groch MW, DePuey EG, Belzberg AC, et al. Planar imaging versus gated blood-pool SPECT for the assessment of ventricular performance: a multicenter study. J Nucl Med 2001; 42: 1773–1779.

19. Groch MW, Marshall RC, Erwin WD, Schippers DJ, Barnett CA, Leidholdt EM Jr. Quantitative gated blood pool SPECT for the assessment of coronary artery disease at rest. J Nucl Cardiol 1998; 5: 567–573.
20. Fischman AJ, Moore RH, Gill JB, Strauss HW. Gated blood pool tomography: a technology whose time has come. Semin Nucl Med 1989; 19: 13–21.
21. Corbett JR, Jansen DE, Lewis SE, et al. Tomographic gated blood pool radionuclide ventriculography: analysis of wall motion and left ventricular volumes in patients with coronary artery disease. J Am Coll Cardiol 1985; 6: 349–358.
22. Moore ML, Murphy PH, Burdine JA. ECG-gated emission computed tomography of the cardiac blood pool. Radiology 1980; 134: 233–235.
23. Daou D, Harel F, Helal BO, et al. Electrocardiographically gated blood-pool SPECT and left ventricular function: comparative value of 3 methods for ejection fraction and volume estimation. J Nucl Med 2001; 42: 1043–1049.
24. Daou D, Coaguila C, Benada A, et al. The value of a completely automatic ECG gated blood pool SPECT processing method for the estimation of global systolic left ventricular function. Nucl Med Commun 2004; 25: 271–276.
25. Van Kriekinge SD, Berman DS, Germano G. Automatic quantification of left ventricular ejection fraction from gated blood pool SPECT. J Nucl Cardiol 1999; 6: 498–506.
26. Nichols K, Humayun N, De Bondt P, Vandenberghe S, Akinboboye OO, Bergmann SR. Model dependence of gated blood pool SPECT ventricular function measurements. J Nucl Cardiol 2004; 11: 282–292.
27. De Bondt P, Nichols K, Vandenberghe S, et al. Validation of gated blood-pool SPECT cardiac measurements tested using a biventricular dynamic physical phantom. J Nucl Med 2003; 44: 967–972.
28. Daou D, Van Kriekinge SD, Coaguila C, et al. Automatic quantification of right ventricular function with gated blood pool SPECT. J Nucl Cardiol 2004; 11: 293–304.
29. Vourvouri EC, Poldermans D, Bax JJ, et al. Evaluation of left ventricular function and volumes in patients with ischaemic cardiomyopathy: gated single-photon emission computed tomography versus two-dimensional echocardiography. Eur J Nucl Med 2001; 28: 1610–1615.
30. Schiller NB, Acquatella H, Ports TA, et al. Left ventricular volume from paired biplane two-dimensional echocardiography. Circulation 1979; 60: 547–555.
31. Schiller NB, Shah PM, Crawford M, et al. Recommendations for quantitation of the left ventricle by two-dimensional echocardiography. American Society of Echocardiography Committee on Standards, Subcommittee on Quantitation of Two-Dimensional Echocardiograms. J Am Soc Echocardiogr 1989; 2: 358–367.
32. Weiss JL, Eaton LW, Kallman CH, Maughan WL. Accuracy of volume determination by two-dimensional echocardiography: defining requirements under controlled conditions in the ejecting canine left ventricle. Circulation 1983; 67: 889–895.
33. Gordon EP, Schnittger I, Fitzgerald PJ, Williams P, Popp RL. Reproducibility of left ventricular volumes by two-dimensional echocardiography. J Am Coll Cardiol 1983; 2: 506–513.
34. Otterstad JE, Froeland G, St John Sutton M, Holme I. Accuracy and reproducibility of biplane two-dimensional echocardiographic measurements of left ventricular dimensions and function. Eur Heart J 1997; 18: 507–513.
35. Popp RL. ASE recommendations. Circulation 1980; 62: 1142–1143.
36. Wright GA, Thackray S, Howey S, Cleland JG. Left Ventricular Ejection Fraction and Volumes from Gated Blood-Pool SPECT: Comparison with Planar Gated Blood-Pool Imaging and Assessment of Repeatability in Patients with Heart Failure. J Nucl Med 2003; 44: 494–498.
37. Germano G, Kiat H, Kavanagh PB, et al. Automatic quantification of ejection fraction from gated myocardial perfusion SPECT. J Nucl Med 1995; 36: 2138–2147.
38. Kim SJ, Kim IJ, Kim YS, Kim YK. Gated blood pool SPECT for measurement of left ventricular volumes and left ventricular ejection fraction: comparison of 8 and 16 frame gated blood pool SPECT. Int J Cardiovasc Imaging 2005; 21: 261–266.
39. Adachi I, Umeda T, Shimomura H, et al. Comparative study of quantitative blood pool SPECT imaging with 180 degrees and 360 degrees acquisition orbits on accuracy of cardiac function. J Nucl Cardiol 2005; 12: 186–194.
40. Hacker M, Stork S, Stratakis D, et al. Relationship between right ventricular ejection fraction and maximum exercise oxygen consumption: a methodological study in chronic heart failure patients. J Nucl Cardiol 2003; 10: 644–649.
41. Slart RH, Poot L, Piers DA, et al. Evaluation of right ventricular function by NuSMUGA software: gated blood-pool SPECT vs. first-pass radionuclide angiography. Int J Cardiovasc Imaging 2003; 19: 401–407.
42. Bacher-Stier C, Muller S, Pachinger O, et al. Thallium-201 gated single-photon emission tomography for the assessment of left ventricular ejection fraction and regional wall motion abnormalities in comparison with two-dimensional echocardiography. Eur J Nucl Med 1999; 26: 1533–1540.
43. Dec GW, Fuster V. Idiopathic dilated cardiomyopathy. N Engl J Med 1994; 331: 1564–1575.

Address for correspondence: Dr. Marcus Hacker, Klinik und Poliklinik für Nuklearmedizin der LMU, Ziemssenstr.1 80336 München, Germany
Tel.: +49-89-51602423; Fax: +49-89-51604555
E-mail: marcus.hacker@med.uni-muenchen.de